Volume 15 | Number 20 | 21 October 2015 | Pages 3955–4100

Lab on a Chip

Miniaturisation for chemistry, physics, biology, materials science and bioengineering

www.rsc.org/loc

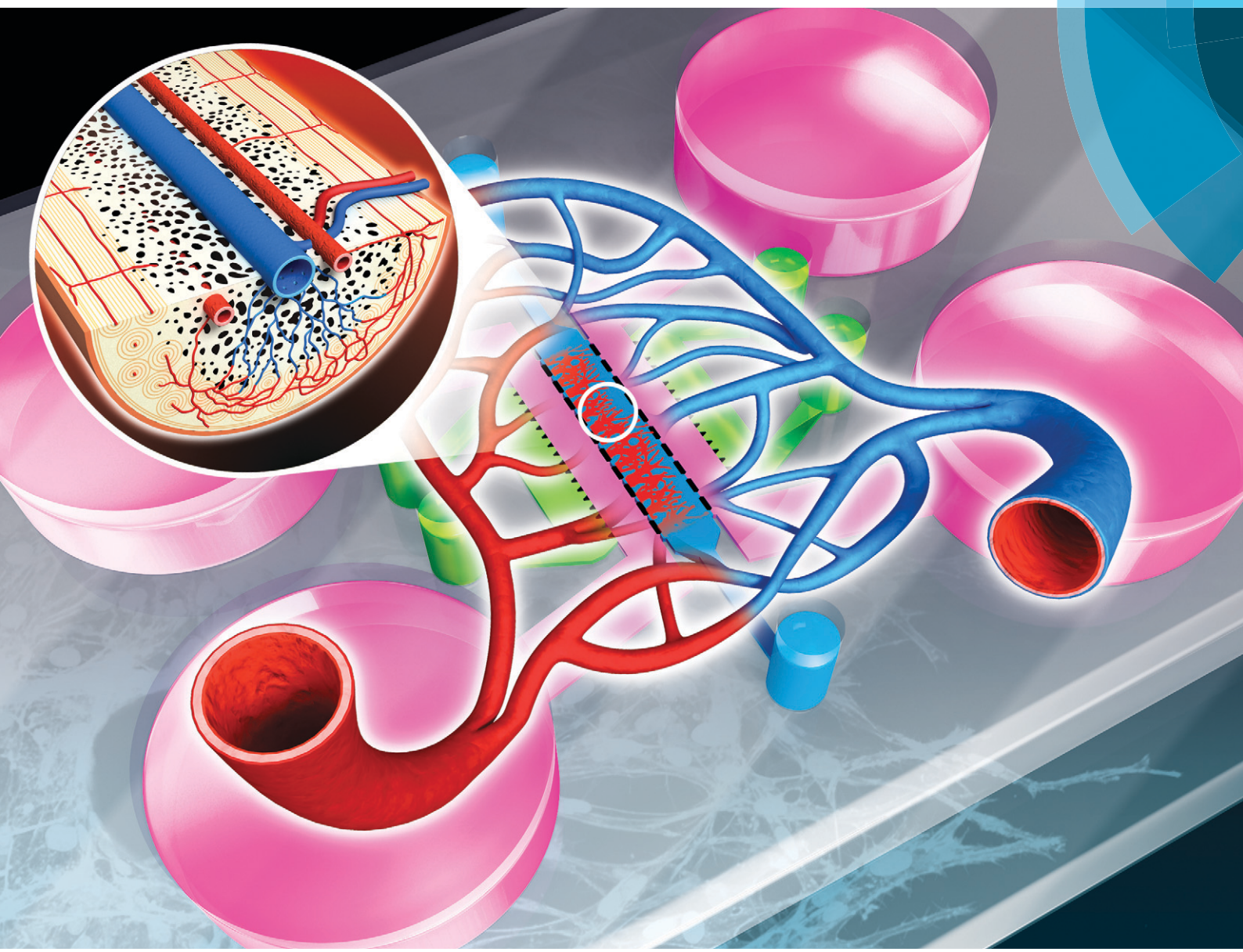

ISSN 1473-0197

ROYAL SOCIETY OF CHEMISTRY

COMMUNICATION

Norhana Jusoh, Soojung Oh *et al.*

Microfluidic vascularized bone tissue model with hydroxyapatite-incorporated extracellular matrix

Lab on a Chip

COMMUNICATION

Microfluidic vascularized bone tissue model with hydroxyapatite-incorporated extracellular matrix†

Norhana Jusoh,‡[ab] Soojung Oh,‡[ac] Sudong Kim,[a] Jangho Kim*[d] and Noo Li Jeon*[ac]

Cite this: *Lab Chip*, 2015, **15**, 3984

Received 22nd June 2015,
Accepted 5th August 2015

DOI: 10.1039/c5lc00698h

www.rsc.org/loc

Current *in vitro* systems mimicking bone tissues fail to fully integrate the three-dimensional (3D) microvasculature and bone tissue microenvironments, decreasing their similarity to *in vivo* conditions. Here, we propose 3D microvascular networks in a hydroxyapatite (HA)-incorporated extracellular matrix (ECM) for designing and manipulating a vascularized bone tissue model in a microfluidic device. Incorporation of HA of various concentrations resulted in ECM with varying mechanical properties. Sprouting angiogenesis was affected by mechanically modulated HA–extracellular matrix interactions, generating a model of vascularized bone microenvironment. Using this platform, we observed that hydroxyapatite enhanced angiogenic properties such as sprout length, sprouting speed, sprout number, and lumen diameter. This new platform integrates fibrin ECM with the synthetic bone mineral HA to provide *in vivo*-like microenvironments for bone vessel sprouting.

Recently, microfluidic devices have been engineered to mimic tissues and organs to model the physiological cellular microenvironment. Further development of these microfluidic models have begun to generate *in vitro* disease (*i.e.* cancer) states for drug screening and understanding of the biological mechanism. Organs-on-chips show great potential as alternatives for replacing animal testing for biomedical, pharmaceutical, and toxicological applications.[1] Consequently, microvascular systems have been proposed as efficient three-dimensional (3D) *in vitro* models for studying complex biological phenomena in living systems.[1,2]

Specifically for vascularized bone tissue models, microfluidic devices have been developed to investigate breast cancer metastasis to the bone and cancer extravasation using an osteo-cell condition microenvironment.[2] *In vitro* platforms of vascularized bone models have also been engineered to evaluate angiogenic potential[3] and for coupling with osteogenesis.[4] For breast cancer bone metastasis, *in vitro* mineralized tumors were developed solely with cancer cells and were able to induce secondary tumor formation.[5] Bone angiogenesis has important roles in endochondral bone formation and repair.[6] However, these *in vitro* methods, either conventional or microfluidic platforms, were not able to mimic the *in vivo* bone angiogenesis that is involved in vessel sprouting within the mineralized bone matrix. Note that an ideal platform for engineering bone tissue should have suitable 3D structures with interconnected pores to facilitate cellular activities while maintaining sufficient mechanical strength to support cell adhesion, proliferation, and differentiation.[7–12]

Here we report a new platform incorporating hydroxyapatite (HA) into a microfluidic chip as a mineralized bone tissue model for mimicking real bone angiogenesis. To this end, fibrin, as a model extracellular matrix (ECM), was combined with HA nanocrystals in order to mimic a real bone tissue matrix with highly porous and interconnected structures of HA–fibrin scaffolds to induce vessel sprouting (Fig. 1). Using this platform, we observed that hydroxyapatite enhanced angiogenic properties such as sprout length, sprouting speed, sprout number, and lumen size.

The microfluidic device consists of four parallel channels separated by 100 μm gaps using microposts, and this also facilitated paracrine communication between endothelial cells (ECs) and stromal cells during vessel formation, as shown in Fig. 1(a–c). Note that we designed channels with 100 μm micropost gaps to prevent leakage and capture the hydrogels in the microfluidic device.[8] Lung fibroblasts (LFs) were selected as stromal cells due to their capability to

[a] *School of Mechanical and Aerospace Engineering, Seoul National University, Seoul, 151-744, South Korea. E-mail: njeon@snu.ac.kr; Tel: +82 2 880 7111*
[b] *Faculty of Biosciences and Medical Engineering, Universiti Teknologi Malaysia, Skudai, Johor, 80990, Malaysia*
[c] *Institute of Advanced Machinery and Design (SNU-IAMD), Seoul National University, Seoul, 151-744, South Korea*
[d] *Department of Rural and Biosystems Engineering, Chonnam National University, Gwangju, 500-757, South Korea. E-mail: rain2000@jnu.ac.kr; Tel: +82 62 530 5181*

† Electronic supplementary information (ESI) available. See DOI: 10.1039/c5lc00698h

‡ These authors contributed equally to this work.

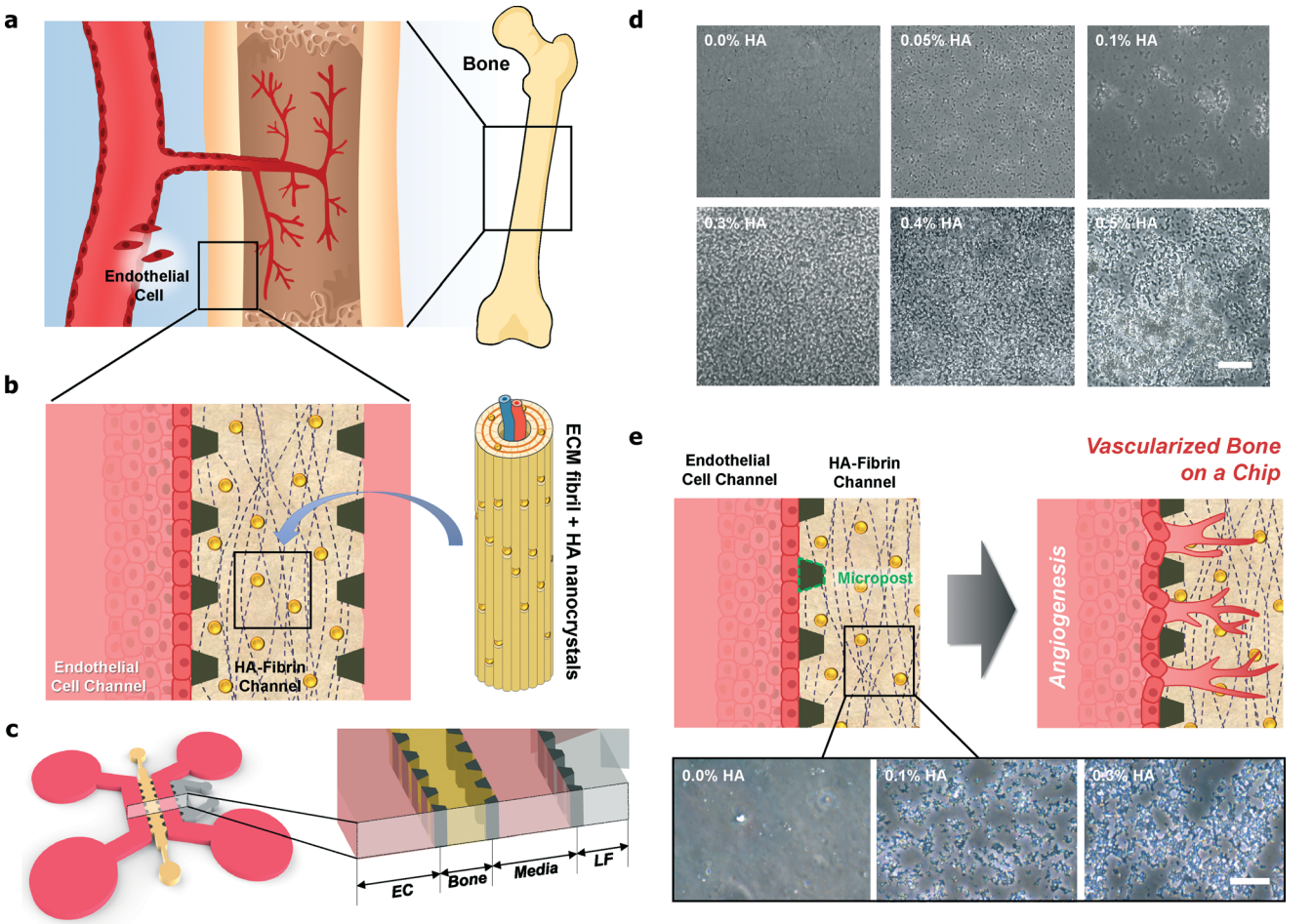

Fig. 1 Rational design and fabrication of microfluidic vascularized bone tissue model with hydroxyapatite-incorporated extracellular matrix (ECM). (a) Angiogenesis during bone development. (b) HA nanocrystals and fibrin ECM encapsulating the blood vessel. (c) Schematic of the microfluidic chip. (d) Images of fibrin incorporated with 0.00%, 0.05%, 0.10%, 0.30%, 0.40%, and 0.50% HA. With 0.5% HA and above, the mixture of fibrin and HA could not polymerize in the microfluidic channel to form hydrogel-like structures. Scale bar: 50 μm. (e) Fibrin and HA polymerization (0.0%, 0.1% and 0.3% HA) after treatment with Trypan Blue. Scale bar: 25 μm.

secrete pro-angiogenic growth factors and ECM proteins that enhance human umbilical vein endothelial cell (HUVEC) morphogenesis.[8] The microfluidics also enable the separation and simultaneous tuning of biomechanical and biochemical simulation, resulting in discrete changes in matrix density, growth factor concentration, and growth factor gradient steepness, which are important during the stages of early sprout initiation, sprout elongation, sprout navigation, and lumen formation.[13]

With HA nanoparticles incorporated in the fibrin ECM, these platforms more closely resemble *in vivo* bone tissue, which is mainly composed of stiff ECM and calcium phosphate minerals that contribute to the hardness and rigidity of the bone. Fig. 1(d) shows various structures consisting of pure fibrin (0% HA) and fibrin with 0.05% HA, 0.10% HA, 0.30% HA, 0.4% HA and 0.50% HA. The images show that the HA particles distributed homogenously within the fibrin hydrogel and the HA particles can be readily seen with increasing HA concentrations in the microfluidic chip (Fig. 1, S1, S2, and Table S1†). We have confirmed that the fibrin and HA polymerization was limited up to 0.4% HA. With 0.5% HA and above, the mixture of fibrin and HA could not polymerize in the microfluidic channel to form hydrogel-like structures, as shown in Fig. 1(d). In addition, to confirm the distribution of HA within the fibrin in the microfluidic channel, we treated the HA–fibrin hydrogel with the hydrophilic dye Trypan Blue[14,15] (Fig. 1(e)). Moreover, Trypan Blue which selectively stained the ceramics was used as a nonspecific indicator of the adsorption potential of HA.[15] As shown in Fig. 1(e), Trypan Blue does not adsorb onto the fibrin hydrogel, but incorporation of HA induces greater dye adsorption on the hydrogel. Thus, incorporation of HA alters protein adsorption.[15]

To confirm the effects of HA on blood vessel formation, we conducted angiogenesis experiments using various HA concentrations. Fig. 2(a) shows examples of bright field images, while Fig. 2(c) shows confocal images of angiogenic vascular networks that were established with 0.0% HA and 0.2% HA. Immunostaining indicates that the expression of the EC marker CD31 was concentrated at junctions between

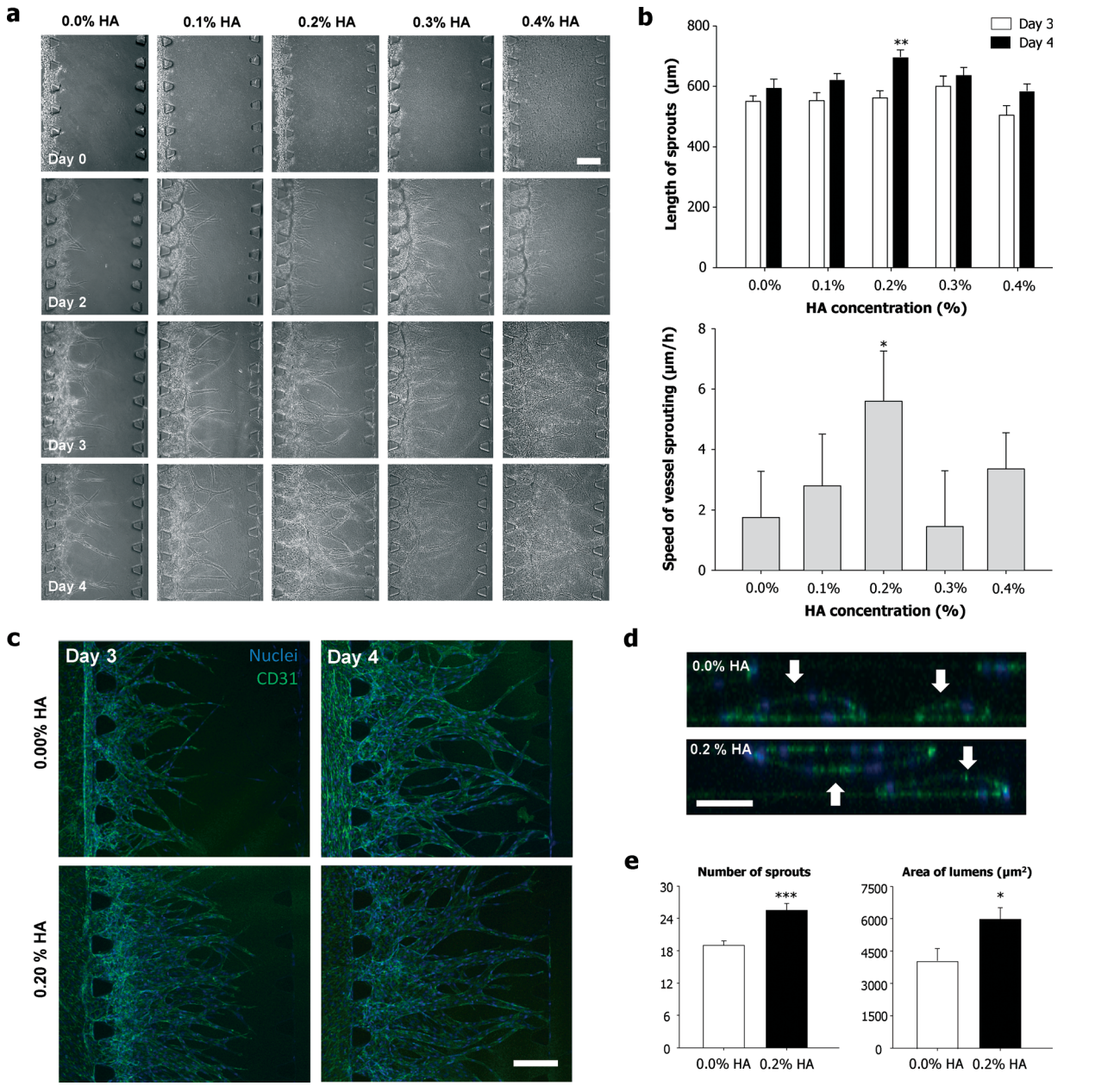

Fig. 2 Enhanced angiogenic processes in microfluidic devices with hydroxyapatite-incorporated extracellular matrix. (a) Bright field images of angiogenic vascular networks established. (b) Quantification of angiogenic sprout growth (n = 20, $P < 0.01$) and average speed of vessel sprouting (n = 20, $P < 0.05$). (c) Confocal images of vascular networks established by angiogenesis that were stained for CD31 (green) and for nuclei (blue). (d) Cross-sectional images of hollow lumens enclosed by HUVECs. (e) Quantification of sprout number at day 4 (n = 20, $P < 0.001$) and area of lumens at day 4 (n = 20, $P < 0.05$). Scale bar: 200 μm. Error bars represent SEM.

adjacent cells. Fig. 2(b) shows the quantification of angiogenic sprout growth for various HA concentrations.

With the addition of HA into the fibrin hydrogel, the average sprout length increased from 593 μm to 694 μm for 0.0% and 0.2% HA, respectively. On the other hand, 0.3% and 0.4% HA slightly decreased the sprout length, which was 635 μm and 585 μm, respectively. Thus, these results suggest that the sprout lengths for 0.0% and 0.4% HA were comparable. Fig. 2(b) shows the average speed of vessel sprouting from day 3 to day 4. Vessel sprouting for 0.2% HA exhibited the fastest speed at 6 μm h^{-1}, followed by 0.4% HA and 0.1% HA with 3 μm h^{-1} for both conditions. For 0.0% HA and 0.30% HA, the sprouting speed was 2 μm h^{-1} and 1 μm h^{-1}, respectively. We have learned that the fibrin gels started to induce fiber aggregation when the HA concentration was increased (*i.e.*, >0.4% HA), resulting in non-uniform hydrogel formation. Therefore, the endothelial cells might penetrate deep into the coarse structures of the hydrogel, which might enhance the angiogenesis speed in the 0.4% HA–fibrin gels as compared with the 0.3% HA–fibrin gels in the microfluidic

devices. Incubation of ECs with crystallized HA favored cell adhesion, spreading, and proliferation, inducing the activation of cytoskeletal architecture without any cytotoxic effect. HA nanocrystals exhibit high biocompatibility for microvascular endothelium, maintaining biochemical markers of healthy endothelium and expressing markers of functional endothelium that might contribute to angiogenesis.

We also determined the effect HA on lumen formation for 0.0% HA and 0.2% HA, as shown in Fig. 2(d) and (e). The average lumen area for 0.2% HA (5963 μm^2) was greater than that for 0.0% HA (4044 μm^2). Fig. 2(e) shows that the number of sprouts at day 4 was 19 and 26 for 0.0% HA and 0.2% HA, respectively. This result suggests that the number of sprouts was increased by the addition of HA into the fibrin. Besides chemical cues such as growth factors, mechanical cues (matrix stiffening) can also effect blood vessel formation, especially during angiogenesis.[16] Hydrogels containing higher HA concentrations were significantly stiffer than the pure hydrogel.[11] Thus, in this work, the fibrin stiffness was tuned by incorporating HA in the hydrogel. ECM stiffness can modulate capillary formation as well as barrier integrity by altering endothelial response to chemical factors.[16] The different values in Fig. 2(e) indicate that lumen formation is more favorable in an HA environment, which is stiffer than pure fibrin. These results are supported by the previous findings that more stable and larger lumens are formed with increasing gel stiffness observed in 3D rigid gels.[13,17] Matrix stiffness also influences EC elongation and sprouting in 3D environments, resulting in enhanced sprouting and outgrowth.[18] In addition, thicker and deeper vessel networks were formed with increasing stiffnesss.[17] Thus, the HA–fibrin stiffness affects the number of sprouting vessels.

Fig. 3 shows a schematic depiction of the proposed model for the effects of HA particles on bone angiogenesis that might be occurring in this study. One of the important factors in developing a bone-mimicking scaffolding material is the ability to favor ECs, which typically occurs *via* growth factors such as vascular endothelial growth factors (VEGFs) that have been reported as critical chemotactic factors for vasculogenesis and angiogenesis. VEGFs are also involved in osteoblast and osteoclast differentiation and appear to enhance bone growth and repair *in vivo*.[19] VEGFs are able to adsorb onto HA nanocrystal surfaces and are able to accelerate angiogenesis.[19,20] There is a strong electrostatic attraction between VEGFs and HAs during the adsorption of VEGFs onto micro- or nanoscale HA surfaces.[20] Therefore, HA has been widely used as a VEGF delivery system. Compared to high concentrations of VEGF release, sustained release of VEGF increased the efficacy of VEGF delivery with prolonged bioavailability of low concentrations of VEGFs, which is more beneficial for bone regeneration.[21] Continuous delivery of low concentrations of VEGFs from calcium phosphate ceramics might increase the efficacy of the administration of VEGFs.[21] Moreover, mesoporous HA (MHA), with various pore sizes, which were infused with VEGFs can gradually release VEGFs and enhance revascularization.[20] Gradual release and accumulation of VEGFs could promote the proliferation of HUVECs and lead to rapid vascularization after implantation.[20] On the other hand, increasing HA concentration will increase growth factor adsorption and will enhance spout formation only up to a certain level. After this optimum level, sprout formation will be reduced with excess HA. High local concentrations of VEGFs result in the formation of malformed and non-functional vessels due to changes in angioblast behavior in normally avascular areas.[22] High local concentrations of VEGFs also cause the loss of individual vessel identity due to alterations in vessel lumen formation and vessel patterning, resulting from the unregulated and excessive fusion of vessels.[22] Furthermore, matrix metalloproteinase (MMP) expression increases with increasing stiffness, resulting in decreasing vessel density.[23] MMPs regulate the vascular structure by degrading elastic fibers and inhibiting angiogenesis by generating angiostatin, which results in the reduction of microvascular density. Taken together, HA particles might play an important role in 3D bone angiogenesis during the bone development process.

Conclusions

Bone is a highly vascularized tissue but lacks a good *in vitro* model that reflects its complex chemical (*i.e.* growth factor trapping) and mechanical (*i.e.* stiffness) microenvironment. We have successfully constructed a bone angiogenesis model in a microfluidic device to overcome the limitations of current *in vitro* models. This new platform integrates fibrin ECM with the synthetic bone mineral HA to provide *in vivo*-like microenvironments for bone vessel sprouting. The formation of angiogenic networks was observed as a function of various

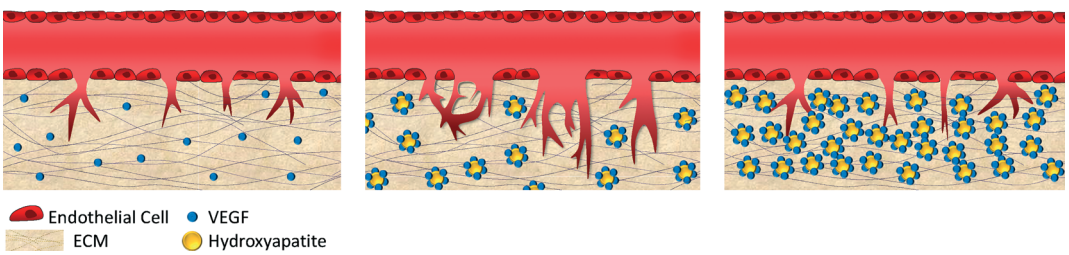

Fig. 3 Schematic depiction of the proposed model for the effects of HA particles on bone angiogenesis. The HA particles might adsorb growth factors (*e.g.*, VEGFs), which might accelerate angiogenesis.[19,20] On the other hand, excessive HA particles might not allow enough space for enhancing angiogenesis.

HA concentrations. This bone angiogenesis platform is relevant for various applications, including drug screening and as a bone disease (*i.e.* metastasis to bone) model. We conclude that our HA-incorporated 3D microvascular networks offer a new approach for the investigation of complex biological phenomena as well as for the analysis of drug responses and toxicities in bone tissues.

Acknowledgements

This work was supported by the Brain Korea 21 Plus Project in 2015 (F14SN02D1310), the National Research Foundation funded by the Ministry of Education (NRF-2015R1A2A1A09005662), the Ministry of Food and Drug Safety in 2015 (15182MFDS455), the Korean Health Technology R&D Project, Ministry of Health & Welfare, Republic of Korea (Grant No. HI14C14000), and a grant (714002-7) from the Agricultural Robotics and Automation Research Center through Agriculture, Food and Rural Affairs Research Center Support Program, Ministry of Agriculture, Food and Rural Affairs.

Notes and references

1 D. Huh, Y. Torisawa, G. A. Hamilton, H. J. Kim and D. E. Ingber, *Lab Chip*, 2012, **12**, 2156.
2 S. Bersini, J. S. Jeon, G. Dubini, C. Arrigoni, S. Chung, J. L. Charest, M. Moretti and M. R. D. Kamm, *Biomaterials*, 2014, **35**(8), 2454.
3 E. Cenni, E. F. Perut and F. N. Baldini, *Acta Pharmacol. Sin.*, 2011, **32**, 21.
4 C. Correia, W. L. Grayson, M. Park, D. Hutton, B. Zhou, X. E. Guo, L. Niklason, R. A. Sousa, R. L. Reis and G. Vunjak-Novakovic, *PLoS One*, 2011, **6**(12), e28352.
5 S. P. Pathi, C. Kowalczewski, R. Tadipatri and C. Fischbach, *PLoS One*, 2010, **5**(1), e8849.
6 (*a*) R. A. Carano and E. H. Filvaroff, *Drug Discovery Today*, 2003, **8**(21), 980; (*b*) M. Kanczle and R. O. C. Oreffo, *Eur. Cells Mater.*, 2008, **15**, 100.
7 Z. Xia, M. M. Villa and M. Wei, *J. Mater. Chem. B*, 2014, **2**, 1998.
8 (*a*) S. Kim, H. Lee, M. Chung and N. L. Jeon, *Lab Chip*, 2013, **13**, 1489; (*b*) J. A. Whisler, M. B. Chen and R. D. Kamm, *Tissue Eng., Part C*, 2013, **20**(7), 543.
9 T. Osathanon, M. L. Linnes, R. M. Rajachar, B. D. Ratner, M. J. Somerman and C. M. Giachelli, *Biomaterials*, 2008, **29**(30), 4091.
10 (*a*) S. Pezzatini, R. Solito, L. Morbidelli, S. Lamponi, E. Boanini, A. Bigi and M. Ziche, *J. Biomed. Mater. Res., Part A*, 2006, **76**(3), 656; (*b*) M. R. Appleford, S. Oh, N. Oh and J. L. Ong, *J. Biomed. Mater. Res., Part A*, 2009, **9**(4), 1019.
11 R. R. Rao, J. Ceccarelli, M. L. Vigen, M. Gudur, R. Singh, C. X. Deng, A. J. Putnam and J. P. Stegemann, *Acta Biomater.*, 2014, **10**, 3091.
12 E. Lammert and J. Axnick, *Cold Spring Harbor Perspect. Med.*, 2012, **2**, a006619.
13 A. Shamloo and S. C. Heilshorn, *Lab Chip*, 2010, **10**, 3061.
14 J. He, D. C. Genetos and J. K. Leach, *Tissue Eng., Part A*, 2010, **16**(1), 127.
15 S. Kim, M. S. Park, O. Jeon, C. Y. Choi and B. Kim, *Biomaterials*, 2006, **27**, 1399.
16 D. J. LaValley and C. A. Reinhart-King, *Advances in Regenerative Biology*, 2014, **1**, 25247.
17 N. Yamamura, R. Sudo, M. Ikeda and K. Tanishita, *Tissue Eng.*, 2007, **13**, 1443.
18 B. N. Mason, A. Starchenko, R. M. Williams, L. J. Bonassar and C. A. Reinhart-King, *Acta Biomater.*, 2013, **9**, 4635.
19 V. Midy, E. Hollande, C. Rey, J. M. Dard and T. Plouee, *J. Mater. Sci.: Mater. Med.*, 2001, **12**, 293.
20 (*a*) C. K. Poh, S. Ng, T. Y. Lim, H. C. Tan, J. Loo and W. Wang, *J. Biomed. Mater. Res., Part A*, 2012, **100A**, 3143; (*b*) Y. Chen, J. Wang, X. Zhu, Y. Fan and X. Zhang, *J. Biomater. Tissue Eng.*, 2014, **4**(2), 155.
21 E. Wernike, M. O. Montjovent, Y. Liu, D. Wismeijer, E. B. Hunziker, K. A. Siebenrock, W. Hofstetter and F. M. Klenke, *Eur. Cells Mater.*, 2010, **19**, 30.
22 C. J. Drake and C. D. Little, *Proc. Natl. Acad. Sci. U. S. A.*, 1995, **92**, 7657.
23 A. W. Y. Chung, H. H. C. Yang, M. K. Sigrist, G. Brin, E. Chum, W. A. Gourlay and A. Levin, *Cardiovasc. Res.*, 2009, **84**, 494.

